

THERMAL ANALYSIS APPLIED TO SOLID CATALYSTS **Acidity, activity and regeneration**

V. J. Fernandes Jr, A. S. Araujo and G. J. T. Fernandes*

Federal University of Rio Grande do Norte, Department of Chemistry, CP 1662
59078-970, Natal, RN, Brazil

Abstract

The use of catalysts in numerous important processes is widespread throughout the chemical and petroleum-processing industries. Thermal analytical techniques can be used to evaluate important properties and processes associated with solid catalysts. This paper presents examples carried out in our laboratory of the general application of TG and DSC to the acidity, activity and regeneration of solid catalysts.

Keywords: acidity, activity, regeneration, solid catalysts, zeolite

Catalyst acidity

Dehydrated zeolites can exhibit both Brønsted and Lewis acid sites, depending on the ion exchange and thermal treatment [1, 2]. The catalysis by acid zeolites is a function of the nature, density and strength of the acid sites, and also the chemistry of the reaction intermediates [3]. Structurally, zeolites comprise a three-dimensional network of SiO_4 and AlO_4^- complexes, linked together through common oxygen atoms [4].

The aim of this work is to evaluate the acid properties of Ca/NaY zeolite by TG and DSC techniques, using *n*-butylamine as the molecular probe. The use of *n*-butylamine for the characterization of solid surfaces such as silica, alumina, silica-alumina and montmorillonite has been reported [5, 6]. The acid strength kinetic parameters are determined by means of the Borchardt-Daniels kinetic model. As the acid properties (strength and total acidity) of zeolite catalysts are related to the activity and selectivity of a number of reactions, measurements of these properties are of interest in catalytic research.

Experimental

Calcium-exchanged NaY zeolite (Ca/NaY) was synthesized by refluxing a NaY zeolite (Si/Al=2.4, determined by atomic absorption spectroscopy) with calcium

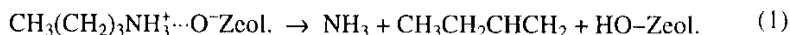
* Author for correspondence: e-mail: valterjr@uol.com.br

chloride solution, followed by thermal treatment at 693 K under a nitrogen flow [7]. The physicochemical characterization of the NaY and Ca/NaY samples was carried out by analytical methods, including ICP-AES, FTIR and XRD patterns. From ICP-AES, the unit cell chemical composition was determined. Structural analysis was performed by Fourier transform infrared spectroscopy, with a Bomem MB-102 instrument. Crystallographic properties of the samples were investigated by X-ray diffraction.

To determine the total acidity, an exchanged sample (0.01 g) previously saturated with *n*-butylamine was transferred to a thermobalance and to a DSC (DuPont 951 and 910, respectively), and submitted to the following programmed thermodesorption isothermal heating at 368 K for 1 h then heating at 15 K min⁻¹ under dry air flowing at 50 cm³ min⁻¹. The total acidity was defined as the absolute mass of base desorbed from the acid sites of the catalyst, expressed in acid sites per g [8].

Results and discussion

To study the acid properties of the Ca/NaY zeolite, it was considered that the basic molecule enters the pores of a zeolite to interact with all the acid sites, and the number of acid sites was determined from the amount of base required to reach the saturation point. The decomposition of *n*-butylamine by the medium and strong acid sites was analyzed. The results from the TG and DTG curves (Fig. 1) revealed that the thermal behaviour of *n*-butylamine–Ca/NaY occurs as follows: (i) desorption of physically adsorbed water and *n*-butylamine before 498 K; (ii) dissociation of the *n*-butylamine from the medium acid sites at 516–676 K, and from the strong acid sites at 676–955 K. The ammonium and butene products of the dissociation of *n*-butylamine are formed by Hoffman degradation [9, 10], as in Eq. (1). This mechanism has also been verified in the decomposition of *n*-butylamine on a silica–alumina catalyst [11].



It is known that primary amines can be converted to diamines over acid catalysts at high temperatures. In the DTG curve, the peak observed in the temperature range

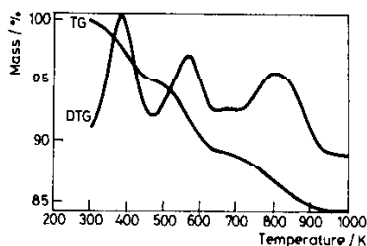
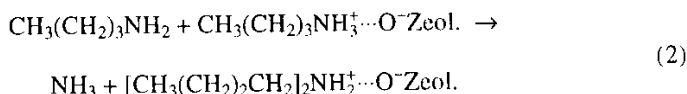


Fig. 1 TG/DTG curves for Ca/NaY zeolite with *n*-butylamine, showing the mass lost from the different acid sites

676–955 K was attributed to the reaction between *n*-butylamine and its protonated form, as shown in Eq. (2):



The presence of butene, ammonia and diamine as products of *n*-butylamine decomposition over acid zeolite catalysts was demonstrated by infrared spectroscopy [12], proton nuclear magnetic resonance [13] and mass spectroscopy [14]. It was suggested that the formation of diamines should occur in the bulk of the Ca/NaY zeolite. However, for calculations of the total acidity of the catalyst, it was assumed that one molecule of *n*-butylamine adsorbs selectively on one acid site.

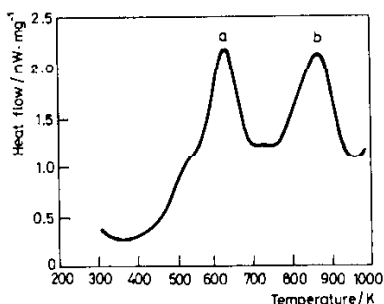


Fig. 2 DSC curve of Ca/NaY zeolite with adsorbed *n*-butylamine, showing exotherms relating to a – medium and b – strong acid sites

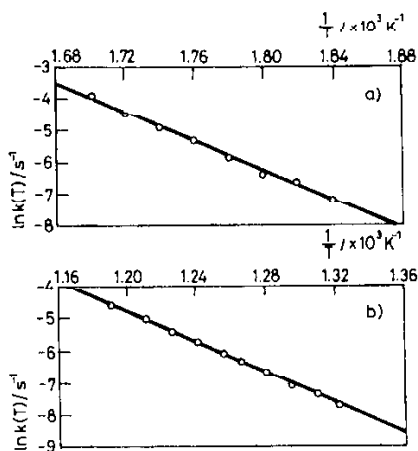


Fig. 3 Arrhenius plots used to determine the activation energy relative to the deamination process from a – medium and b – strong acid sites

The DSC curve of the Ca/NaY zeolite (Fig. 2) displayed two exothermic peaks, relating to each acid site strength. The first peak corresponds to the desorption of *n*-butylamine and probable dissociation of the base from the medium acid sites, according to Eq. (3), whereas the second is related to the decomposition of the amine from the strong acid sites. It is suggested that the enthalpies and activation energies relating to each process are directly proportional to the acid site strength in each specific temperature range.

Table 1 Acid site density and strength kinetic parameters of Ca/NaY zeolite

Parameter	Acid sites	
	Medium	Strong
	TG/DTG	
Total acidity (acid sites per g)·10 ²⁰	7.8	7.0
Temperature range/°C	243–403	403–682
	DSC/Borchardt-Daniels kinetic model	
Reaction order	2.8	1.8
Activation energy/kJ mol ⁻¹	195.8	211.0
Heat of reaction/J g ⁻¹	238.2	371.5
	From TG and DSC data	
Acid strength/(J per acid sites)·10 ⁻¹⁹	3.0	5.3

Based on the Borchardt-Daniels kinetic model [15], software developed by DuPont was used to determine the kinetic parameters of *n*-butylamine desorption from the Ca/NaY zeolite. In this way, curves were plotted that depicted the time conversion (min) as a function of temperature (K) and $\ln k(T)$ as a function of inverse temperature (1/K). The time conversion curves represent the desorption and degradation of *n*-butylamine as concerns the acid sites of different strengths. The $\ln k(T)$ vs. $1/T$ plot results in a straight line, as illustrated in Figs 3(a) and 3(b). The activation energies of the deamination process referring to the two exotherms can be obtained from the slopes of the straight lines, demonstrating that the Borchardt-Daniels kinetic model can be applied for evaluation of the relative acid strength in solid acids [6]. The total acidity (from TG/DTG) and kinetic parameters (from DSC) relating to the desorption of *n*-butylamine from the medium and strong acid sites are given in Table 1.

Catalyst activity

The degradation of waste synthetic polymers has been at the focus of increased attention because of their potential use as fuels or chemical sources [16, 17]. Additionally, the recycling of polymers from waste products can contribute to the solution of pollution problems. The use of suitable catalysts can enhance the thermal degradation of synthetic polymers [18, 19], which may be monitored by thermogravimetry [20, 21].

In this example, the degradation of high-density polyethylene (HDPE) was processed in the presence of HZSM-5 zeolite and the results of catalytic and thermal degradations were compared.

Experimental

The HZSM-5 was obtained by exchanging ZSM-5 (synthesized by the hydrothermal method) with ammonium chloride and subsequent calcination at 823 K for 4 h.

HDPE in powder form was obtained from Palmman (Brazil) as BM012. Blending of polymer and catalyst previously activated at 723 K for 4 h was performed in a ball mill. The catalyst concentration was 10% (m/m). Polymer degradation was carried out in a quartz microreactor at 723 K, under a static nitrogen atmosphere. The sample mass was 1 g. Two different samples were studied under these conditions: HDPE alone (PE1) and HDPE mixed with HZSM-5 zeolite (PE2).

The reactor was connected online to an HP 5890-II gas chromatograph equipped with a flame ionization detector and an HP-5 capillary column (30 m).

Sample degradation was also investigated with a Perkin-Elmer Delta 7 Thermobalance, from room temperature to 800°C, at heating rates of 5.0, 10.0 and 20.0 K min⁻¹. The thermogravimetric analyses were conducted in a dynamic atmosphere of nitrogen (30 cm³ min⁻¹). 5 mg of sample was used for each experiment.

Results and discussion

Thermogravimetric analysis

Although reactions conducted in bulk involve more serious problems of heat transfer than those observed in the TG of small samples, the influence of the catalyst on HDPE degradation can readily be explored by carrying out thermogravimetric experiments, which allow useful internal comparisons. Thus, the loss in mass of the mixture (polymer+zeolite) was measured as a function of temperature up to 800°C, and the results were compared with those obtained without catalyst. Through the use of differential TG curves, it was possible to determine T_i , T_m and T_f , which are the temperatures corresponding to the initial mass loss, the maximum rate of mass loss, and the final constant mass, respectively, reported in Table 2. It was observed that the presence of the HZSM-5 zeolite led to a marked lowering of T_i , T_m T_f .

Table 2 Values of T_i , T_m and T_f observed in thermogravimetric analysis of HDPE without and with catalyst, in a dynamic nitrogen flow of 30 cm³ min⁻¹

Sample	T_i , °C	T_m , °C	T_f , °C
PE1	361.9	462.0	491.7
PE2	274.1	390.6	424.8

Degradation mechanism

Standard solutions containing C₅-C₃₀ n-alkanes were analyzed on the same column and under the same conditions. The retention times (RTs) of these hydrocarbons were used as references in order to group the degradation products. We designated as F5 the

fraction containing all the products with *RTs* up to that of *n*-pentane. F6 was the fraction containing all the products with *RTs* between those of *n*-pentane and *n*-hexane, and so on.

Chromatographic analysis revealed that the thermal degradation of HDPE without catalyst gave rise to products distributed over a wide range of carbon atom number (C₅–C₂₆) as reported in Table 3; the main fraction involved C₁₀–C₁₅ (60.2%). The catalytic reaction led to lighter products (C₅–C₂₆), predominantly C₅–C₉ (73.5%). This behaviour may be due to the strong acid sites of HZSM-5 zeolite, which can promote polymer chain cracking.

Table 3 Product distribution (m%) in the degradation of HDPE without and with catalyst, in a static nitrogen atmosphere

Fraction	PE1	PE2
F5	0.618	23.05
F6	6.60	16.94
F7	3.82	11.06
F8	4.11	11.81
F9	5.94	10.67
F10	8.70	8.41
F11	9.28	6.39
F12	9.30	4.84
F13	9.20	3.39
F14	9.26	2.07
F15	8.20	1.08
F16	6.21	0.290
F17	4.77	–
F18	3.32	–
F19	3.29	–
F20	2.72	–
F21	1.95	–
F22	1.20	–
F23	0.771	–
F24	0.502	–
F25	0.212	–
F26	0.027	–

Kinetic study

The activation energy was calculated for polymer degradation with and without catalyst, using dynamic integral TG curves at several heating rates, as proposed by

Ozawa [22] and Flynn and Wall [23]. Software based on these methods was used to treat the TG data, allowing an evaluation of the apparent activation energy E via the expression

$$E = -18.2 \frac{\delta \log \beta}{\delta(1/T)} \quad (3)$$

where β is the heating rate and T is the absolute temperature.

The activation energy observed for the polymer degradation without catalyst was $170.2 \text{ kJ mol}^{-1}$ against 67.0 kJ mol^{-1} in the presence of HZSM-5 zeolite. These results indicate that the zeolite may have acted as a cracking catalyst for HDPE, enhancing the generation of light products of potential industrial use, probably due to the Brönsted and Lewis strong acid sites of the zeolite.

Catalyst regeneration

One of the main causes of catalyst deactivation is the formation and deposition of coke [24], which results from the nucleation of non-reactive polymeric species on the catalyst surface, blocking the channels and cages [25]. Catalyst regeneration is generally achieved by gradual heating under an oxidizing atmosphere [26].

In this work, a thermogravimetric method is proposed for study of the kinetic parameters of zeolite regeneration. The technique, which makes use of integral thermogravimetric curves, was optimized by means of microprocessed integrated mathematical methods. The kinetic parameters obtained from the TG curves are activation energy, rate constants, half-lifetimes and, in particular, the coke removal time as a function of temperature.

Experimental

The H-Y zeolite was synthesized by refluxing NaY zeolite with ammonium chloride solution, followed by calcination at 773 K under a nitrogen flow. The chemical composition of the sample was $\text{Na}_{19.4}\text{H}_{37.6}(\text{AlO}_2)_{57}(\text{SiO}_2)_{135}$, determined by atomic absorption spectroscopy.

The H-Y zeolite catalyst, which is a white powdery solid, was used in the alkylation of benzene with dodecene in a fixed-bed continuous flow reactor at 573 K, with a WHSV (weight hourly space velocity) of 23.5 h^{-1} . Under these conditions, after 1 h, the HZSM-5 zeolite catalyst had become deactivated by coking.

To study the regeneration of the coked catalyst, a DuPont 951 thermobalance was calibrated over all heating rates, using a gas purge, under the same conditions as for analysis.

Samples of the deactivated catalyst (containing 27.7 m% of coke) were submitted to pre-treatment under a dry air atmosphere at 303 K. They were then heated in the temperature range 303–1273 K at heating rates of 2.5, 5.0, 10 and 20 K min^{-1} , with a controlled dry air flow of $120 \text{ cm}^3 \text{ min}^{-1}$. 0.01 g of coked zeolite was used for each experiment, and all experiments were repeated three times.

Results and discussion

Toop [27] developed a relationship to estimate the lifetime of a polymeric material as a function of temperature, demonstrating that it is possible to calculate the activation energy relating to the thermal degradation of a polymer by using the slope of the logarithmic heating rate curves as a function of reciprocal temperature. This method has been used to evaluate the thermal stability of rigid polyurethane [28], and in studies on coke thermoxidation for solid catalyst regeneration [29, 30].

Toop [27] determined a relationship between the activation energy E and the estimated lifetime for several polymeric coatings:

$$T_c = \frac{E/R}{\ln t_c - \ln \left[\frac{E}{\beta R} P \left(\frac{E}{RT_p} \right) \right]} \quad (4)$$

where t_c is the estimated lifetime, β is the heating rate, E is the activation energy, T_c is the temperature to which the system is exposed, R is the gas constant and T_p is the temperature at which the mass loss is 5% [$=f(\beta)$].

A plot of this equation shows that a small increment in the oxidation temperature causes a drastic decrease in the time required for catalyst regeneration. Blaine [31] formulated a correlation between the Toop and the Flynn-Wall methods in software form, whereby the lifetimes of different polymeric materials can be determined. The program was used for data processing in respect of the thermoxidation of coked H-Y zeolite.

The first step in the TG curve, from 303 to 587 K, is due to hydrocarbon adsorbed during the alkylation reaction (Fig. 4).

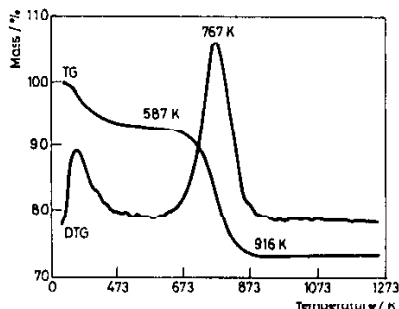


Fig. 4 Thermogravimetric (TG) and differential thermogravimetric (DTG) curves of coked H-Y zeolite. Heating rate 10 min^{-1} , dry air flow $120 \text{ cm}^3 \text{ min}^{-1}$

In order to determine accurately the temperature range of coke thermoxidation, the second step in the TG and DTG curves was utilized for each heating rate. For example, with a β value of 10 K min^{-1} , the thermoxidation of coke occurs from 587 to 916 K (Fig. 4).

It may be noted that the thermal region of coke removal is a direct function of the temperature gradient in the samples and is directly proportional to the heating rate employed (Fig. 5), which must be considered in pilot plant estimation. These curves relating to the experiments were reproducible.

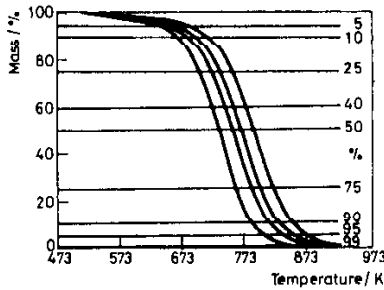


Fig. 5 Multiple heating rate thermogravimetric integral curves for different coke removal rates (in %). From left to right: 2.5, 5.0, 10 and 20 K min⁻¹

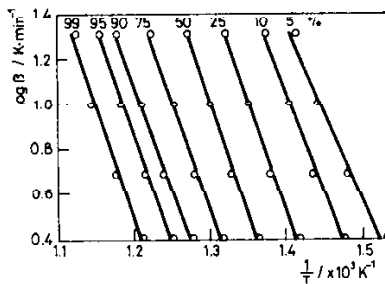


Fig. 6 Logarithm of heating rate vs. reciprocal temperature for different coke removal rates (in %). Activation energy is determined by differentiating these curves

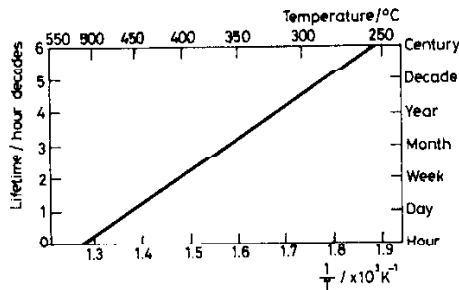


Fig. 7 Theoretical regeneration time of coked H-Y zeolite vs. temperature

The linearity observed when the logarithm of heating rate is plotted as a function of reciprocal temperature for several degradation rates of coke (Fig. 6) confirms that the adopted kinetic model can be used to evaluate the removal of char coating (coke) from catalysts. From the first derivative of these curves, the activation energy E is determined as being $183.1 \text{ kJ mol}^{-1}$.

From the relationship of Toop [27], it is possible to plot lifetime vs. regeneration temperature, which allows a prediction as to how long the removal of coke will take for a given temperature (Fig. 7). This relation can be applied only to the temperature range between 303 and 1000 K because sintering of the catalyst may occur at higher temperatures [32]. For instance, it was observed that, to remove 99% of coke from zeolite in a period of 1 h, it would be necessary to carry out thermoxidation at 791 K, with a dry air purge flow of $120 \text{ cm}^3 \text{ min}^{-1}$.

Conclusions

TG was used to quantify the acid site density of the catalyst and, combined with DSC, to estimate acid site strength. Thermogravimetry was also employed to determine the kinetic parameters of polyethylene catalytic degradation and the optimal conditions for thermoxidation of coke deposited on the catalyst surface. The presented examples, where TG and DSC were employed to determine zeolite acidity, activity and regeneration, demonstrate that thermal analysis can be used as a useful tool for solid catalyst evaluation.

* * *

This work was supported by Conselho Nacional de Desenvolvimento Científico e Tecnológico (CNPq).

References

- 1 J. W. Ward, *J. Catal.*, 11 (1968) 259.
- 2 P. A. Jacobs, *Carboniogenic Activity of Zeolites*. Elsevier Amsterdam, 1977, p. 2
- 3 S. Csicsery, *Zeolites*, 4 (1984) 202.
- 4 R. Carvajal, P. Chu and J. H. Lunsford, *J. Catal.*, 125 (1990) 123.
- 5 T. Morimoto, J. Imai and M. Nagao, *J. Phys. Chem.*, 78 (1974) 704.
- 6 R. Bezman, *J. Catal.*, 68 (1981) 242.
- 7 A. S. Araujo, D. Sc. Thesis, Universidade de São Paulo, São Paulo Brazil, 1992.
- 8 A. S. Araújo, V. J. Fernandes Jr., I. Giolito and L. B. Zinner, *Thermochim. Acta*, 223 (1993) 29.
- 9 P. A. Jacobs and Uytterhoeven, *J. Catal.*, 26 (1972) 175.
- 10 L. M. Parker, D. M. Bibby and J. Patterson, *Zeolites*, 4 (1984) 168.
- 11 M. Takahashi, Y. Iwasawa and S. Ogasawara, *J. Catal.*, 45 (1976) 15.
- 12 A. K. Gosh and G. Curthoys, *J. Chem. Soc. Faraday Trans. I*, 80 (1984) 99.
- 13 J. Mochida, A. Yasutake, H. Fujitsu and K. Takeshita, *J. Catal.*, 82 (1983) 313.
- 14 L. M. Parker, D. M. Bibby and R. H. Meinhold, *Zeolites*, 5 (1985) 384.
- 15 H. Borchardt and F. Daniels, *J. Amer. Chem. Soc.*, 79 (1956) 41.
- 16 W. Kaminski, J. Janning and H. Sinn, *Eur. Rubber J.*, 15 (1979) 161.
- 17 R. C. Poller, *J. Chem. Tech. Biotechnol.*, 30 (1980) 152.
- 18 A. Lucchesi, G. Maschio and P. Giusti, *Poliplast*, 288 (1981) 73.

- 19 G. Audisio, A. Silvani, P. L. Beltrame and P. Cartini, *J. Anal. Appl. Pyrol.*, 7 (1984) 83.
- 20 Y. Uemichi, Y. Kashiowaya, M. Tsukidate, A. Ayame and H. Kanoh, *Bull. Chem. Soc. Jpn.*, 55 (1983) 2768.
- 21 Y. Uemichi, Y. Kashiowaya, A. Ayame and H. Kanoh, *Chem. Lett.*, 1 (1984) 41.
- 22 T. Osawa, *Bull. Chem. Soc. Jpn.*, 38 (1965) 1881.
- 23 J. H. Flynn and W. A. Wall, *Polym. Lett.*, 4 (1969) 323.
- 24 R. Hughes, *Deactivation of Catalysts*, Academic Press London, 1984, p. 3.
- 25 P. Magnoux, M. Guisnet, S. Mignard and P. Cartraud, *J. Catal.*, 117 (1989) 495.
- 26 P. G. Menon, *J. Mol. Catal.*, 59 (1990) 207.
- 27 D. T. Toop, *IEEE Trans. Electr. Insul.*, EI-6 (1), 1971.
- 28 V. J. Fernandes Jr., D. Sc. Thesis, Universidade de São Paulo, 1991.
- 29 V. J. Fernandes Jr. and A. S. Araújo, *Química Nova*, 18 (1995) 11.
- 30 V. J. Fernandes Jr. and A. S. Araújo, *Thermochim. Acta*, 255 (1995) 273.
- 31 R. L. Blaine, DuPont Thermal Application Brief, TA 84 (1980).
- 32 J. A. Rabo, *Zeolite Chemistry and Catalysis*, ACS Monograph 171, American Chemical Society Washington, 1976, p. 323.